

Measuring Galactic Cosmic Rays and Secondary Particles with the Radiation Assessment Detector

B. EHRESMANN¹, C. ZEITLIN¹, D. M. HASSLER¹, R. F. WIMMER-SCHWEINGRUBER², S. BÖTTCHER², D. E. BRINZA³, J. GUO², J. KÖHLER², C. MARTIN², S. RAFKIN¹, THE RAD SCIENCE TEAM, AND THE MSL SCIENCE TEAM

¹ Southwest Research Institute, Boulder Colorado, USA

² Institute for Experimental and Applied Physics, Christian-Albrechts-Universität zu Kiel, Germany

³ Jet Propulsion Laboratory, California Institute of Technology, Pasadena, California, USA

ehresmann@boulder.swri.edu

Abstract: Since the landing of the Curiosity rover on Mars, the Radiation Assessment Detector (RAD) onboard the Mars Science Laboratory (MSL) has been measuring the energetic particle radiation environment on the Martian surface. This environment mainly consists of two parts: Galactic Cosmic Rays (GCRs) propagating through the Martian atmosphere to the surface, and secondary particles created by interactions of the primary GCRs and the Martian atmosphere and soil. RAD also successfully measured the radiation environment in the spacecraft on MSL's cruise to Mars. There, the radiation environment was dominated by GCRs, but interactions with the surrounding material of the spacecraft created a non-negligible contribution of secondary particles. Also, five Solar Energetic Particle events were observed during cruise. RAD is designed to distinguish between neutral and charged particles. Charged particles are further distinguished between those that stop in the detectors and those that penetrate. In this presentation, we will give an overview of the RAD instrument and present results of charged particle measurements during the cruise phase.

Keywords: RAD, MSL, cosmic rays, charged particles.

1 The Radiation Assessment Detector (RAD)

The Radiation Assessment Detector (RAD) [1] is an energetic particle detector onboard NASA's Mars Science Laboratory (MSL) mission. RAD uses a combination of silicon and scintillation detectors to characterize the charged and neutral radiation environment on the Martian surface and in space on the trip to Mars. As of this writing, RAD has measured almost continuously during the 253-day cruise phase to Mars and the first \sim 300-sols on the Martian surface.

The main science objective of RAD is the assessment of the measured radiation environment to define radiation hazards and health risks for future manned missions to the red planet. Detailed knowledge of the radiation field can also aid to analyze its influence on any potential simple life forms (e.g., bacteria) that might reside in a dormant state beneath the Martian surface. Furthermore, measured particle spectra are a valuable asset in validating current particle transport models, both for the radiation environment on Mars (where RAD is the first ever particle detector to measure on the surface) and in space during cruise.

Figure 1 shows a schematic of the RAD sensor head (RSH). The RSH consists of 5 detectors for particle measurements: 3 silicon detectors (labeled A, B, C in the schematic), a CsI scintillator (D), and a plastic scintillator (E). Additionally, the D and E detectors are surrounded by an anti-coincidence (AC), also consisting of a plastic scintillator (F). RAD is designed to measure both neutral and charged particles. For neutral particle detection, the instrument makes use of the D and E detectors and the AC. In contrast to charged particles, neutrals (neutrons and γ -rays) have a high likelihood to be measured in the detectors without creating a signal in the AC. As D and E further have different effi-

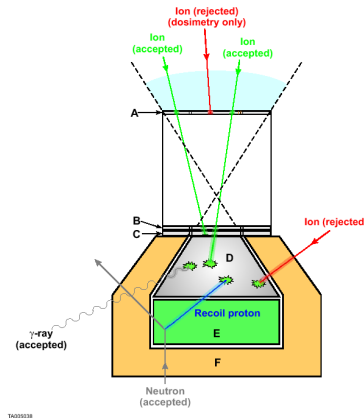


Figure 1: Schematic of the RAD sensor head. The green arrows show allowed flight paths for stopping charged particles. The red arrows indicate charged particles that are rejected.

ciencies for neutron and γ -ray detection, RAD can also distinguish between these neutral particle types. This, however, requires a complicated inversion method, e.g. as described in [2].

2 Charged particle detection with RAD

Here we focus on RAD's capabilities for detecting charged particles. We distinguish between penetrating and stopping particles. Penetrating particles are defined as depositing energy in all detectors (A, B, C, D, E), as well as the bottom

part of F, while a particle is classified as stopping when it makes a signal in at least A and B, but not in the AC, yielding an allowable flight path from the upper hemisphere, constricted by the opening angle of the A and B telescope ($\sim 30^\circ$). The actual categorization of these event classes requires a more elaborate logic as described in [3].

As the maximum energy a stopping charged particle can deposit depends on the particle's charge, mass, and energy, different ions have different stopping energies. Table 1 shows such stopping energies for a selection of ion species. Here, these energies were calculated by analyzing simulations of interactions of particles and a model of the RAD sensor head, conducted with the Monte-Carlo code GEANT4 [4].

Ion species	Max. stopping energy
Proton	110 MeV
Helium	110 MeV/nuc
Carbon	190 MeV/nuc
Oxygen	220 MeV/nuc
Iron	420 MeV/nuc

Table 1: Estimated maximum energy deposits for ions stopping in RAD.

A thorough analysis of the charged particles measured by RAD requires the ability to accurately identify particles. As seen in figure 2, making use of a variation of the “Goulding”-method [5] we are able to distinguish stopping particles by their ion species and in some cases by their masses. Since stopping particles deposit all of their initial energy

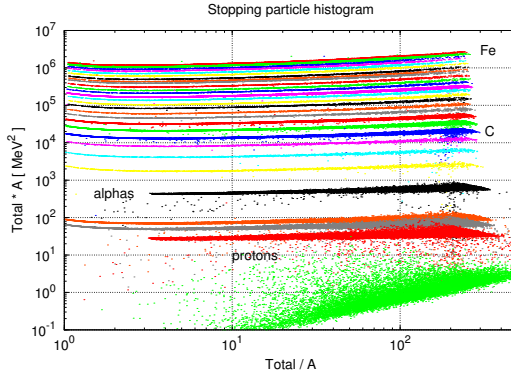


Figure 2: GEANT4 simulation of stopping particles in RAD. Shown are starting from the bottom: electrons (green), protons (red), deuterons (grey), tritons (orange), helium (black), and further ions with charges of $3 \leq Z \leq 26$.

in the detectors, we are able to provide differential fluxes of different ion species for measurements during the cruise phase or on the Martian surface.

As there is no information on the total energy of penetrating particles derivable, we instead provide integral fluxes for these particles. Figure 3 shows that it is still possible to identify different ion species of penetrating particles.

3 Radiation environment during cruise

RAD measured the radiation environment inside the spacecraft for 220 days of the 253-day cruise from Earth to

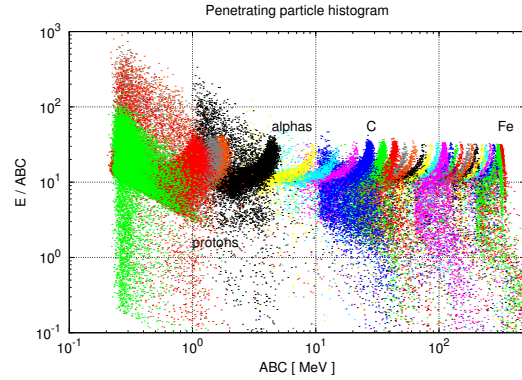


Figure 3: GEANT4 simulation of penetrating particles in RAD. Shown are starting from the left: electrons (green), protons (red), deuterons (grey), tritons (orange), helium (black), and further ions with charges of $3 \leq Z \leq 26$.

Mars. Because the Sun was relatively quiet during MSL’s cruise, the radiation field consisted almost exclusively of contributions from Galactic Cosmic Rays (GCRs) and secondaries produced in the shielding that surrounded RAD. Figure 4 shows a polar plot of the shielding depth above RAD’s upwards-directed Field-Of-View (FOV) during the cruise phase. The model yields an average shielding of

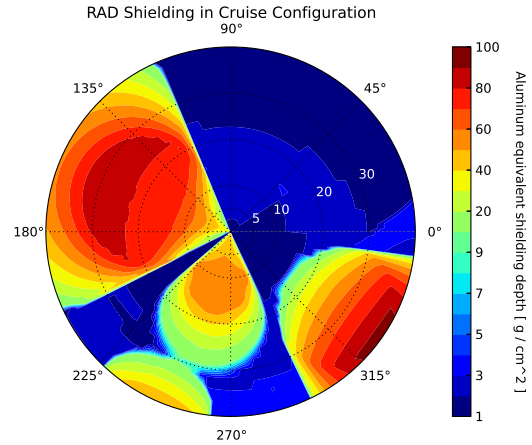


Figure 4: Polar plot of the shielding mass above RAD’s FOV during the cruise phase. The shielding model was produced by Shawn Kang of the Jet Propulsion Laboratory (JPL) in Pasadena, CA, using a CAD model of the spacecraft. Adapted from [6].

$\sim 22.5 \text{ g/cm}^2$ aluminum-equivalent depth above the FOV made up of the inner segment of RAD’s A and the B detector.

All said, the measured flux is not a precise representation of the GCR flux but – assuming similar shielding mass for future manned missions – might provide valuable insight on the radiation to be encountered on such a mission.

4 Proton-to-deuteron ratio

First results of RAD measurements during the cruise phase were published recently [6]. There, we reported the dose and dose equivalent measured by RAD using the B and E detectors, and the LET distribution recorded in the B

detector. Dose and dose equivalent are integral quantities in the sense that they represent sums over the measured spectra. Some details are lost in the integrations. The spectra themselves contain more information.

We are particularly interested in the question of whether existing models can accurately predict the fluxes of secondary particles in shielded environments. A straightforward test can be made using the measured ratio of protons to deuterons in the RAD cruise data; a preliminary analysis is presented here, largely for illustrative purposes.

The flux of deuterons in the primary GCR is known to be small [7]. At low energies (below 96 MeV for protons and 65 MeV/nuc for deuterons), these particles can be identified in RAD by their unique signatures in, for instance, a scatter plot showing the ratio of the total amount of energy deposited in all detectors versus the energy deposited in detector A on the x-axis and the total energy deposit times the deposit in A on the y-axis. An example of this configuration is shown in Figure 2. For both particle types, the total energy is assumed to simply be the sum of the measured energies; for deuterons, this sum is divided by 2 to obtain the energy per nucleon. For a given bin of energy per nucleon, we take the ratio of the number of protons to the number of deuterons to obtain the ratio, which is plotted as a function of energy per nucleon in Figure 5, along with a prediction for this energy range made with the OLTARIS [8] model. In the OLTARIS calculation, the

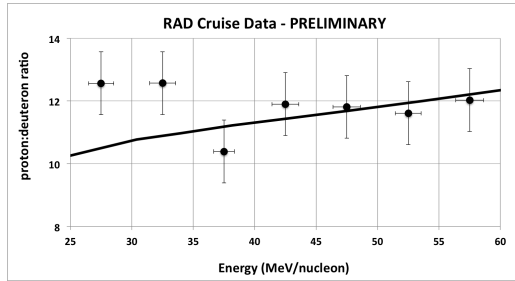


Figure 5: Preliminary proton-to-deuteron ratio as measured by RAD during the cruise phase (data points). The solid line shows the prediction by the OLTARIS model.

time period was taken to be the first six weeks of RADs cruise, a period when operation of the instrument was stable and there were no solar events that would affect the ratio. OLTARIS uses the 2010 version of the Badhwar-ONEill model [9] to determine the solar modulation parameter, and calculates GCR fluxes accordingly. The error bars on the data points shown in Figure 5 are statistical only. The data are consistent with the ratio being energy independent; the weighted average of the data is 11.7 ± 0.4 (χ^2 of 3.9 with 5 degrees of freedom). In contrast, the model predicts a modest increase in the ratio of about 20% over this energy range. Given the statistical uncertainties, one can draw either rising or falling lines through the data points and stay within all error bars. However, the measurements below 35 MeV/nuc are inconsistent with the prediction at about the 2σ level.

The proton-to-deuteron ratio is one of many possible tests that can be performed with the RAD cruise data. Agreement between the measured ratio and the OLTARIS prediction is reasonable above 35 MeV/nuc, but at lower energies the data suggest the model may need fine-tuning. In this instance, the deviation of the model from the data would

have negligible impact on integral quantities such as dose or dose equivalent, but this does not obviate the need to further pursue this and similar tests.

5 Conclusions

RAD obtained a richly detailed data set during MSLs cruise to Mars, and continues to obtain high-quality data on the surface of Mars. Work is in progress to make detailed comparisons of particle spectra to model predictions for both the cruise and surface radiation environments. A simple example was presented here showing reasonable - but not perfect - agreement with the NASA-Langley OLTARIS model. Additional tests against a variety of other models are forthcoming.

6 Acknowledgements

RAD is supported by NASA (HEOMD) under JPL subcontract #1273039 to Southwest Research Institute and in Germany by DLR and DLR's Space Administration grant numbers 50QM0501 and 50QM1201 to the Christian-Albrechts-Universität zu Kiel. A portion of this research was carried out at the Jet Propulsion Laboratory, California Institute of Technology, under a contract with the National Aeronautics and Space Administration. We thank Shawn Kang at the Jet Propulsion Laboratory, California Institute of Technology, for his work on the shielding model for RAD during the cruise phase. We greatly appreciate discussions with our colleagues, especially Günther Reitz, Thomas Berger, and Daniel Matthiä, at the German Aerospace Center (DLR) in Cologne, Germany.

References

- [1] Hassler, D. M., et al., *Space. Sci. Rev.* 170 (2012) 503-558 doi:10.1007/s11214-012-9913-1.
- [2] Köhler, J., et al., *Nuclear Instruments and Methods in Physics Research B* 269 (2011) 2641-2648 doi:10.1016/j.nimb.2011.07.021.
- [3] Ehresmann, B., PhD thesis, CAU Kiel, Germany (2012).
- [4] Agostinelli, S., et al., *Nucl. Instrum. Methods A* 506 (2003) 250-303.
- [5] Goulding, F. S., Harvey, B. G., *Annual Review of Nuclear and Particle Science* 25 (1975) 167-240 doi:10.1146/annurev.ns.25.120175.001123.
- [6] Zeitlin, C., et al., *Science* 340 (2013), 1080-1084, doi:10.1126/science.1235989.
- [7] Myers, Z. D. et al., *Adv. Sp. Res.* 35 (2005) 151-155 doi:10.1016/j.asr.2003.10.050.
- [8] Singleterry, Jr., R. C., et al., *Acta Astronautica* 68 (2011) 1086-1097.
- [9] O'Neill, P. M., *IEEE Trans. Nucl. Sci.* 57 (2010) 3148-3153 doi:10.1109/TNS.2010.2083688.